Fabrication and Characterization of TiO_2:rGO Thin Films on Si Substrate by Spin coating technique for the Determination of Sensitivity of Methanol Gas Concentration

G. Prabhavathi[1,2], A. Mohamed Saleem[1,3] , A. Ayeshamariam[1,2*], N.Punithevelan[4], M. P. Srinivasan[4], and M. Jayachandran[5]

[1]Research and Development Center, Bharathidasan University, Tiruchirappalli, India.

[2*] Department of Physics, Khadir Mohideen College, Adirampattinam, India.

[3]Department of Physics, Jamal Mohamed College (Auto), Tiruchirappalli, India.

[4]Department of Physics Division, School of Advanced Sciences (SAS), VIT University Chennai Campus, Chennai, India.

[5]Department of Physics, Sethu Institute of Technology, Pullor, Kariapatti, India.

***Corresponding author Email: aismma786@gmail.com**

Abstract - This work the fabrication, characterization and application of nanostructured TiO_2 doped with 1 Wt% of reduced grapheme oxide thin films on interdigitated silver electrodes grown on SiO_2/Si substrates. The TiO_2 doped with 1 Wt% of reduced graphene thin films were synthesized on silicon wafer using a Spin coating technique. Two different mother solutions were prepared by dissolving TiO_2 in methanol and isopropanol in presence of monoethanolamine as a stabilizer and graphene oxide NPs reduced from Amla Juice was in another beaker to dope. The AFM, XRD and FTIR characterization revealed that both the thin films were composed of Cubic crystals of nanoscale dimensions. However, the TiO_2:rGO doped derived thin films were more homogeneous and were composed of smaller sized TiO_2 crystals. The TiO_2:rGO doped thin films on Si Substrate was used to determine the sensor applications.

Keywords - Sensor, Spin coating technique, Si substrate and TiO_2:rGO

I. INTRODUCTION

Nanostructured rGO doped with TiO_2 thin film has been intensively studied because of its semiconducting properties, broad band gap, high lattice constant. It has been successfully applied in biomedical sensors[1-2], chemical and gas sensors[3-4], ultraviolet light sensors[5-7], light-emitting diodes (LEDs) [8], solar cells and other optoelectronic devices. We explored here a Spin coating technique because of its low-cost, low temperature annealing and chemical compositional control and feasibility for large scale production of desired dimension films on a variety of substrates [9].

The TiO_2:rGO thin films were fabricated on thermally oxidized p-type silicon (100) wafer with interdigitated electrodes (IDE) and were characterized using field emission scanning electron microscope (FESEM, Hitachi SU-70),X-ray diffractometer (XRD, Bruker D8), and Fourier transform infrared spectroscopy (FTIR, Perkin Elmer 400).Finally, the TiO_2:rGO coated .

II. EXPERIMENTAL

Silicon dioxide (SiO_2) on silicon (Si) wafer was used as a substrate in this project. Silver (Ag) Interdigitated electrodes (IDE)were then fabricated on SiO_2/Si substrate. Prior to the growth of SiO_2 on silicon wafer, the plane wafer was ultrasonically cleaned by immerging into acetone and isopropanol (IPA). Approximately 180-nm thick Si layer was produced on the cleaned wafer using a wet oxidation process. Interdigitated Ag electrodes were fabricated on the Si substrate using a thermal evaporator. TiO_2 seed solutions which were later coated on the Si were prepared by dissolving 1Wt% doped rGO with 99% of TiO_2 [TiO_2: rGO] into methanol. The aged TiO_2 solution

 DOI : 10.18231/2454-9150.2018.1346

was deposited onto the sensor device by using a Spin coating technique at a speed 3000 rpm for 20 s. The deposition process was repeated for 3 times as to get a thicker TiO_2: rGO thin film. These processes depend up on the optimized substrate temperature resulting into the perfect decomposition of the precursors. Though the all other parameter like NSD, air flow, spray rate, precursors concentration have been kept constant and the quantity of the solution has influenced the properties TiO_2: rGO thin film [10].

For each deposition process, spin coated TiO_2: rGO thin films were dried at 150°C for 20 min to remove the organic residuals that might exist on the TiO_2: rGO thin films. The topography of the TiO_2: rGO thin films were studied using a Atomic Force Microscopy (AFM) with roughness. The XRD spectrum of TiO_2:rGO thin films were recorded at room temperature using a X-ray diffractometer. To confirm the chemical bonding and tetragonal structure of the TiO_2: rGO thin films, Fourier transform infrared (FTIR) spectroscopy was performed. Methhanol with different concentration in *(ppm)* was tested to find the sensitivity of TiO_2: rGO thin films [11].

III. RESULTS AND DISCUSSION

The X-ray diffraction measurements were carried out to study the crystalline quality and crystallographic orientation of the TiO_2 : rGO thin films on Si substrate and the spectra are shown in Figure 1 and its values are shown in Table 1. All the diffraction peaks were matched with the TiO_2 : rGO thin films on Si substrate standard card (JCPDS 89-4203), demonstrating the formation TiO_2 crystals. The sharp and narrow diffraction of the peaks it demonstrated that all TiO_2 : rGO thin films on Si substrate were of good crystalline in quality. This X-ray diffraction data is used to determine dimensions of unit cell, crystal structure, texture coefficient, standard deviation and crystallnity. The grain size of the crystallite is calculated using Scherrer's formula (1) [12],

$$D = \frac{k\lambda}{\beta.\cos\theta} \qquad \text{-------(1)}$$

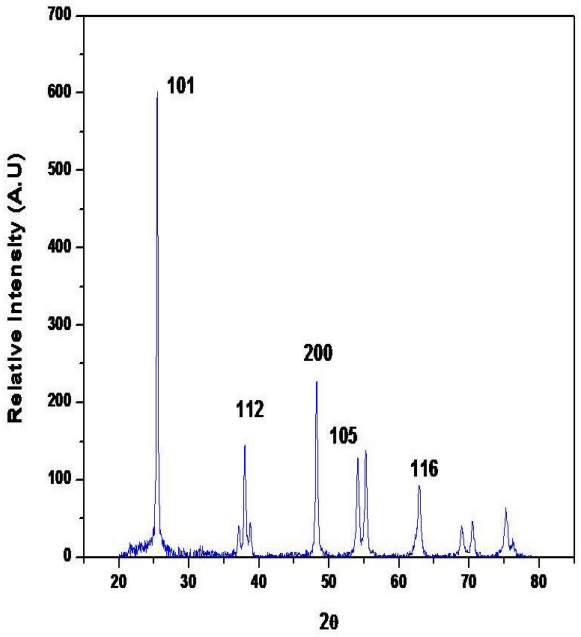

Figure 1 XRD analysis of TiO_2 : rGO thin films

Table -1 Structural Properties of TiO_2 : rGO thin films

TiO_2 : rGO thin films on Si Substrate	2Θ (Std)	2Θ (Obs)	d(Std)	d (Obs)	Crystal Size (nm)	Lattice constant **JCPDS 89-4203** Aº	Lattice Constant Aº (Obs)
101	25.304	25.475	3.5169	3.49652	34.71	a=3.785	a = 3.810
200	48.037	48.256	1.8925	1.88596	40.59	c= 9.514	c= 9.112

The reflection peaks with high intensities at (101), (110) indicated that the TiO_2: rGO thin films was of tetragonal structure. The results suggested that the crystal growth orientation of TiO_2:rGO thin films from highest peak at 25.306°, which was on (101) plane. However, the TiO_2:rGO thin films provided the highest diffraction peak at 25.454, which was on (110) plane. Thus both planes demonstrated the pure wurtzite hexagonal structure of TiO_2: rGO thin thin films. It also reflected that all the TiO_2: rGO thin films had c-axis orientation. The XRD results also reflected for the TiO_2: rGO thin films having average crystal size of 37 nm had different morphology and crystal growth orientation, correlating the AFM findings [13]. The surface morphology of TiO_2:rGO thin films prepared was studied using a AFM and is given in Figure 2(a-c). The resultsdemonstrated that both solutions resulted in TiO_2:rGO particles with hexagonal morphology.

 DOI : 10.18231/2454-9150.2018.1346

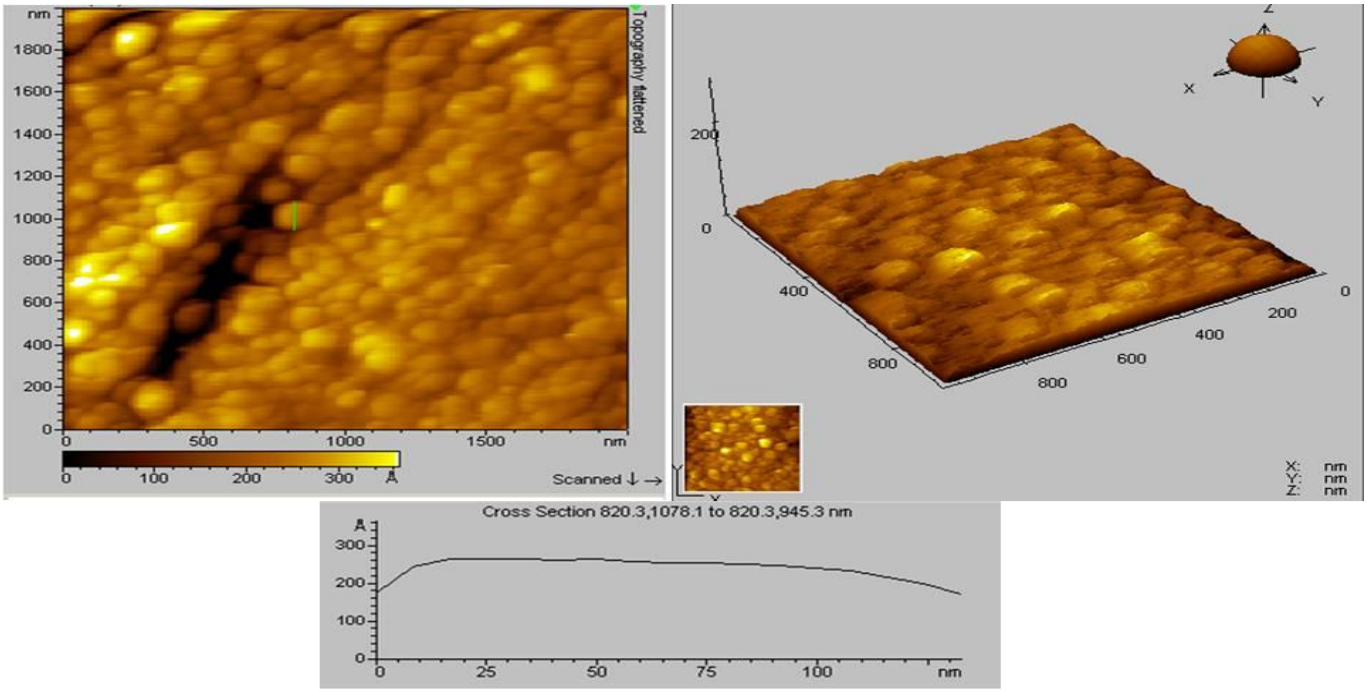

Figure 2(a-c) 2D, 3D and roughness of TiO_2:rGO on Si Subtrate

These XRD also showed that these films were of tetragonal structure, strongly correlating the AFM and FTIR investigation results. The nanocrystallite size in Si layers and its distribution depends on the etching current density. The initiation of silicon etching a 5 mA/cm^2 with larger grains. The etching process at 10 mA/cm^2 has produced surface hillocks, possibly generated from the removal of silicon leaving this non-uniform nanostructures. The horizontal cross section shows a pore diameters of about 3.6 µm formed at a high current density of 60 mA/cm^2 [14].

The chemical bonding, compositional quality and functionalities of TiO_2: rGO a peak at 693 cm^{-1} was due to the existence of the local vibration of the substitution Titanium with carbon in the Si crystal lattice. The broad band observed at 1240 cm^{-1} was assigned to the C-H mode vibration. Whereas the sharpest peak at 1695cm^{-1} and 2356 cm^{-1} was assigned to the stretching frequency of Si bond [15].

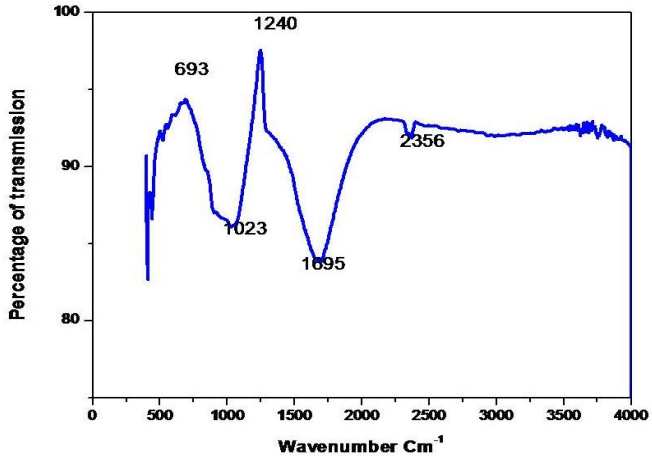

Figure 3. FTIR Analysis of TiO_2:rGO thin films on Si susbtrate

Total volume of the glass chamber is 15ml and is provided with a 3 inlets for injecting the gas inside the chamber through a peristaltic pump. Sensors either in the porous pellet or thin films forms were mounted on a special holder which was placed inside the chamber through a port. The sensor holder has provision to make electrical contacts with other devices. The sensor holder also houses a thermocouple for accurate measurement of the temperature of the sensor [16].

The temperature of the sensor was controlled at the desired temperature. There is a PID controlled heater and substrate holder for thin film sensor measurement is placed inside the chamber. In the present investigation, the heater itself acts as the sample holder which suits for different types of base substrates like tube, matrix plates, etc. The chamber is made with stainless steel and the heater also with the same metal to conduct the elevated temperatures. An air tight septum is used to keep the vacuum condition throughout the sensor studies. The sensing action of a semiconducting oxide sensor material towards an analyte gas is measured in terms of the variation in the conductance of the material and the parameter measured is the resistance of the material present either as thin films or as porous pellet. A typical experiment to measure the sensing characteristic of the sensor towards an analyte gas is described [17].

 DOI : 10.18231/2454-9150.2018.1346

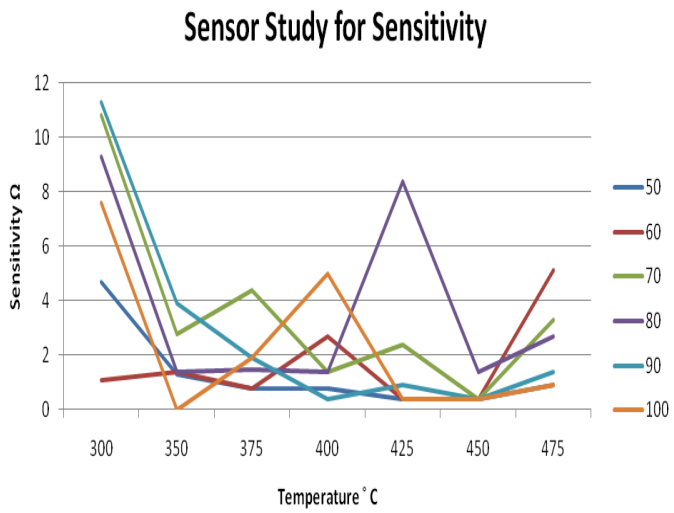

Figure 4 Sensitivity of TiO_2:rGO thin film on Si substrate at different substrate temperatures for 50 to 100 *ppm* of methanol concentration

Adequate quantity of the analyte gas is then injected into the test chamber so that resulting concentration is in the desired concentration level in air (*ppm*). Change in resistance of the thin film is measured as a function of time till a steady value is reached. The chamber is then purged with air and the sensor is allowed to reach the initial value of the resistance before the next experiment is carried out [18].

Substrate is placed on the substrate holder. A thermocouple is fixed inside the chamber, touching the extreme end of the steel rod thereby recording the temperature inside the furnace. A PID controller maintains a constant relationship between the applied temperature and real time temperature.

Peristaltic pumps work by compressing and relaxing a hose that's positioned between a rotating device and circular pump housing. Most peristaltic pumps use rigid shoes that rub and torque the hose. Vector uses rotating rollers that provide the same push with far less hose wear [19].

Fluid positioned ahead of the rollers gets pushed forward as the rollers rotate inside the case. Meanwhile, the portion of the hose just behind the rollers rebounds to create a vacuum. This draws fluid into the pumping hose, which is then pushed forward by the rollers. The peristaltic method employed by Vector can create 100% compression at all times, with zero slipping and incredibly accurate metering while producing up to 20-feet of suction lift.

Sensitivity curve was shown in Figure 4 when the Si substrate temperatures varies from 300 to 475º C for the different methanol concentration of 50 *ppm* to 100 *ppm* [20].

IV. CONCLUSION

Nanostructured TiO_2:rGO thin films on Si susbtrate by using Spin coating technique. The XRD, AFM and FTIR characterization revealed that the thin films were composed of tetragonal TiO_2:rGO thin film on Si substrate of this TiO_2:rGO crystals of nanoscale dimensions. The sensitivity of the film is nearly 8 for 80 ppm with temperatures from 400 to 425º C. Size reduction of the grains in an TiO_2:rGO thin film on Si substrate gas-sensitive material leads to operating temperatures 400-425º C, higher sensitivity, and less reliance on methanol gas concentration. Size reduction of heater elements in turn leads to a lower overall power budget, faster heating and cooling.

REFERENCES

[1]. Hemangi, B. and Nikhita, K., 2016. People Counting System Using Raspberry Pi With Opencv. at International Journal for Research in Engineering Application & Management (IJREAM), ISSN, pp.2494-9150.

[2]. Feng, W.Y., Chiu, N.F., Lu, H.H., Shih, H.C., Yang, D. and Lin, C.W., 2008. Surface plasmon resonance biochip based on ZnO thin film for nitric oxide sensing. Journal of Bionanoscience, 2(1), pp.62-66.

[3]. Skubal, L.R., Meshkov, N.K. and Vogt, M.C., 2002. Detection and identification of gaseous organics using a TiO_2 sensor. Journal of Photochemistry and Photobiology A: Chemistry, 148(1-3), pp.103-108.

[4]. Ayeshamariam, A., Saravanakkumar, D., Kashif, M., Sivaranjani, S. and Ravikumar, B., 2016. Analysis on the effect of ZnO on Carbon nanotube by spray pyrolysis method. Mechanics of Advanced Materials and Modern Processes, 2(1), p.3.

[5]. Saravanakkumar, D., S. Sivaranjani, K. Kaviyarasu, A. Ayeshamariam, B. Ravikumar, S. Pandiarajan, C. Veeralakshmi, M. Jayachandran, and M. Maaza. "Synthesis and characterization of ZnO–CuO nanocomposites powder by modified perfume spray pyrolysis method and its antimicrobial investigation." Journal of Semiconductors 39, no. 3 (2018): 033001.

[6]. Ayeshamariam, A., Kashif, M., Bououdina, M., Hashim, U., Jayachandran, M. and Ali, M.E., 2014. Morphological, structural, and gas-sensing characterization of tin-doped indium oxide nanoparticles. Ceramics International, 40(1), pp.1321-1328.

[7]. Kaviyarasu, K., N. Geetha, K. Kanimozhi, C. Maria Magdalane, S. Sivaranjani, A. Ayeshamariam, J. Kennedy, and M. Maaza. "In vitro cytotoxicity effect and antibacterial performance of human lung epithelial cells A549 activity of zinc oxide doped TiO2 nanocrystals:

 DOI : 10.18231/2454-9150.2018.1346

investigation of bio-medical application by chemical method." Materials Science and Engineering: C 74 (2017): 325-333.

[8]. Akyildiz, I.F., Su, W., Sankarasubramaniam, Y. and Cayirci, E., 2002. A survey on sensor networks. IEEE communications magazine, 40(8), pp.102-114.

[9]. Mejrjardi, H.A., Rezaei-Zarrchi, S. and Aisha, A., 2009, J. Iran. Chem. Soc., Vol. 6, Suppl., pp. S151-S202.

[10]. Mao, C., Solis, D.J., Reiss, B.D., Kottmann, S.T., Sweeney, R.Y., Hayhurst, A., Georgiou, G., Iverson, B. and Belcher, A.M., 2004. Virus-based toolkit for the directed synthesis of magnetic and semiconducting nanowires. *Science*, *303*(5655), pp.213-217. [11]. Kim, S.O., Solak, H.H., Stoykovich, M.P., Ferrier, N.J., de Pablo, J.J. and Nealey, P.F., 2003. Epitaxial self-assembly of block copolymers on lithographically defined nanopatterned substrates. Nature, 424(6947), p.411.

[12]. Pinna, N., Neri, G., Antonietti, M. and Niederberger, M., 2004. Nonaqueous synthesis of nanocrystalline semiconducting metal oxides for gas sensing. Angewandte Chemie International Edition, 43(33), pp.4345-4349.

[13]. Salehi, A., 2002. Selectivity enhancement of indium-doped SnO2 gas sensors. *Thin Solid Films*, *416*(1-2), pp.260-263.

[14]. Wang, H.T., Kang, B.S., Ren, F., Tien, L.C., Sadik, P.W., Norton, D.P., Pearton, S.J. and Lin, J., 2005. Hydrogen-selective sensing at room temperature with ZnO nanorods. Applied Physics Letters, 86(24), p.243503..

[15]. Wang, C., Chu, X. and Wu, M., 2006. Detection of H2S down to ppb levels at room temperature using sensors based on ZnO nanorods. *Sensors and Actuators B: Chemical*, *113*(1), pp.320-323.

[16]. Catto, A.C., da Silva, L.F., Ribeiro, C., Bernardini, S., Aguir, K., Longo, E. and Mastelaro, V.R., 2015. An easy method of preparing ozone gas sensors based on ZnO nanorods. Rsc advances, 5(25), pp.19528-19533.

[17] Ionescu, R., Hoel, A., Granqvist, C.G., Llobet, E. and Heszler, P., 2005. Low-level detection of ethanol and H_2S with temperature-modulated WO_3 nanoparticle gas sensors. Sensors and Actuators B: Chemical, 104(1), pp.132-139.

[18]. Rothschild, A. and Komem, Y., 2004. The effect of grain size on the sensitivity of nanocrystalline metal-oxide gas sensors. *Journal of Applied Physics*, *95*(11), pp.6374-6380.

[19]. Shimizu, Y. and Egashira, M., 1999. Basic aspects and challenges of semiconductor gas sensors. Mrs Bulletin, 24(6), pp.18-24.

[20]. Vernat-Rossi, V., Garcia, C., Talon, R., Denoyer, C. and Berdagué, J.L., 1996. Rapid discrimination of meat products and bacterial strains using semiconductor gas sensors. *Sensors and Actuators B: Chemical*, *37*(1-2), pp.43-48.

 DOI : 10.18231/2454-9150.2018.1346